Developing a Timed Navigation Architecture for Hospital Delivery Robots

Jorge B. Silva
Industrial Electronic Department
University of Minho
Guimares, Portugal
Email: jbruno@dei.uminho.pt

Cristina Santos
Industrial Electronic Department
University of Minho
Guimares, Portugal
Email: cristina@dei.uminho.pt

João Sequeira
Instituto Superior Tecnico
Lisboa, Portugal
Email: jseq@isr.ist.utl.pt

***Abstract*—In hospitals, typical tasks of delivering goods between different locations are usually done by auxiliary staff. With the development of robotic technologies, such tasks can be performed by mobile robots releasing the staff effort to other tasks. In order to successfully complete the tasks of delivering goods inside hospitals, mobile robots should be able to generate trajectories free of collisions. In addition, including timing constraints to the generated trajectories has not been addressed in most current robotic systems, and it is critical in robotic tasks as human-robot interaction. Including timing constraints means to obey to the planned movement time, despite diversified environmental conditions or perturbations. In this paper we aim to develop a navigation architecture with timing constraints based on a mesh of nonlinear dynamical systems and feedthrough maps for wheeled mobile robots. A simulated hospital environment and a wheeled robot pioneer 3-DX are used to demonstrate the robustness and reliability of the proposed architecture in cluttered, dynamic and uncontrolled hospital scenarios.**

I. INTRODUCTION

Typical tasks of delivering goods between different locations within hospitals are usually done by auxiliary staff, wasting human efforts that could be used to provide better patient care. With the development of robotic technologies, such tasks can be performed by mobile robots releasing the auxiliary staff to other tasks. However, to carry out tasks of delivering goods inside hospitals, mobile robots should be able to generate trajectories free of collisions. In general, the control architectures of mobile robots that can perform delivering tasks should include a set of different models namely: world modeling, global planning and local planning. Each model addresses a particular function allowing to efficiently plan the required free-collision trajectory. However, a more relevant problem arises in the trajectory planning problem if temporal stabilization of the generated movements is considered. Temporal stabilization means to obey to the planned movement, despite diversified environmental conditions or perturbations. In practical terms, any movement of the mobile robot should be compensated for when perturbations or environment conditions either hold up, accelerate or decelerate the respective movement. If the robot takes longer than expected to complete its task because of unpredicted disturbances, the change of timing should be compensated by the acceleration of the robot along its trajectory.

The temporal stabilization is well suited for hospital environments, especially if we consider tasks requiring human-robot interaction, *i.e.* if someone of the hospital staff calls for a robot, it has to delivery goods within a specified time $MT(\mathrm{s})$. The major advantage of controlling the movement time of the robot is to achieve a better scheduling of the delivery tasks and therefore improving the staff organization of the hospital. In this paper we aim to develop a navigation architecture with timing constraints based on a mesh of nonlinear dynamical systems and feedthrough maps for wheeled mobile robots. Our novelty does not focus on each individual module of the architecture but in their integration with the timing constraints.

II. STATE OF THE ART

Recent research has shown that there are several works aiming at developing robust, flexible and reliable control systems for autonomous mobile robots making them able to navigate in hospital environments for delivery tasks, TUG [5], RoboCart [2], HelpMate [7], Swisslog's Transcar [4], Matsushita's HOSPI [1], SpeciMinder [3], MKR [17] and iWard [16]. These robots can move in hospitals, and additionally they also can perform a wide range of delivery tasks and other related activities. However, they do not address the generation of timed trajectories for the delivery tasks.

To the best of our knowledge, the generation of timed trajectories embedded in feedback structures remains an open problem, that has received little attention both in robotics and in neuroscience. Typical approaches in literature for generating timed controls are based on the dynamical system theory, as a consequence of the several advantages provided by this theory [13]. Herein, related research concerning to timed trajectories has been verified in several scopes such as: learning by demonstration [9], movements for biped and quadruped location [12], rehabilitation [10] and movement for wheeled robots [11],[15].

III. DYNAMICAL SYSTEMS BASED ARCHITECTURE

The overall architecture of our system (fig. 1) is hierarchically divided into three subsystems of control: global, local and timing, and based on a mesh of nonlinear dynamical systems and feedthrough maps. Each subsystem is in charge of a specific function and each one works independently of the others. However, information flows among them.

The global control is responsible for providing the direction ψ_{tar} that the robot should follow during a task to reach the global goal location P_g. The local control receives the direction ψ_{tar} at each time step and verifies through the robot's sensorial

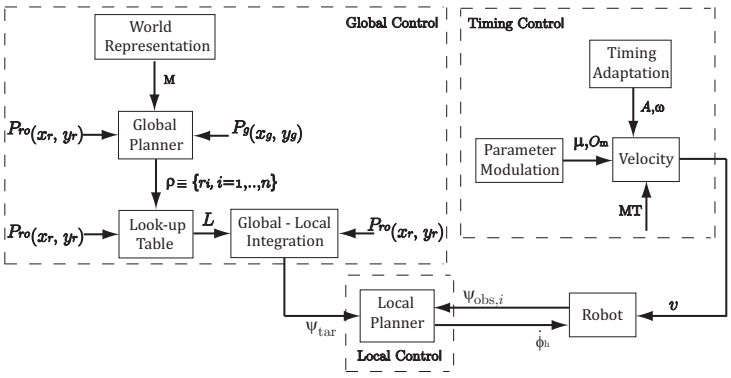

Fig. 1. Schematic of the overall architecture containing a global, a local and a timing control.

information if this direction can be followed by the robot, or if there are obstacles obstructing such direction. A nonlinear dynamical system (see [6]) is used to merge the obstacle avoidance and goal seeking contributions and to provide the direction $\phi_{\rm h}$, that the robot has to follow. The timing control is responsible for generating the suitable velocity v that makes the robot to complete successfully its task within the specified time frame, $MT\,(\mathrm{s})$, through the Landau-Stuart oscillator (see for instance [15]). Conditions for the stability of this navigation architecture were already derived by applying nonlinear analysis and control theory viewpoints [14].

A. Global Control

In the global control, four individual modules are responsible for converting the information of the environment's structure into the direction $\psi_{\rm tar}$ that the robot should follow. However, note that this direction does not take into account unexpected obstacles that are on the environment.

The world representation adopts a common strategy in robotics to represent the environment through a topological map, consisting in a set of regions, where each region r_i represents a room or a corridor of the environment (see [18] for a detailed explanation). Regions result from a tessellation procedure on the environment and a transition function M is enough to represent such regions.

Based on the transition function M, the global planner aims at finding a sequence of regions $\rho \equiv \{r_i, i = 1,\ldots,n_{\rm a}\}$ connecting the perceived position of the robot P_{ro}, to a neighborhood of the goal location $\mathfrak{B}(P_g,\varepsilon)$ for an adequate radius ε, where P_g is the position of the goal location provided to the robot by the user. Note that in practical terms, the robot's position P_{ro} is perceived with a maximum error τ and it can be represented as a circle centered at the robot's real position $P_r(x,y)$ with a radius τ.

The Look-up Table is a feedthrough map responsible for ensuring a correct transition between the regions in ρ by providing a line segment L that defines the border line between the region where the robot is, r_i, and the next region r_{i+1}.

The global - local integration module receives the selected line segment L that contains the point $P_i(x_i,y_i)$ that the robot has to follow to move from region r_i to region r_{i+1} and has as extremities the points $P_{1i}(x_{1i},y_{1i})$ and $P_{2i}(x_{2i},y_{2i})$ obtained from the environment. Point P_i is the solution (x_i,y_i) of the following dynamical system through the projection of the current position of the robot P_{ro} onto the line L and passing by points $P_{1i}(x_{1i},y_{1i})$ and $P_{2i}(x_{2i},y_{2i})$,

$$\dot{x}_i = \lambda_{\rm tr}\left(x_i - x_{1i} + u(x_{2i} - x_{1i})\right), \quad (1)$$

$$\dot{y}_i = \lambda_{\rm tr}\left(y_i - y_{1i} + u(y_{2i} - y_{1i})\right), \quad (2)$$

where u is the distance between P_i and P_{ro} and $\lambda_{\rm tr}$ defines the relaxation rate of the dynamical system. Then, P_i is used to set the reference direction for the robot, $\psi_{\rm tar}(\mathrm{rad})$, in order to move from region r_i to region r_{i+1},

$$\psi_{\rm tar} = \arctan\left(\frac{y_i - y_r}{x_i - x_r}\right). \quad (3)$$

B. Local Control

The local control contains the module responsible for setting the direction that the robot has to follow at each instant of time, $\phi_{\rm h}$, by taking into account the direction $\psi_{\rm tar}$ and the direction where obstacles are present $\psi_{{\rm obs},i}$. $\phi_{\rm h}$ is ruled by the dynamical systems approach (see [6]) defined as,

$$\dot{\phi}_{\rm h} = \sum_{i=1}^{n_s}\left(-\lambda_{{\rm obs},i}(\phi_{\rm h} - \psi_{{\rm obs},i})\exp\left[-\frac{(\phi_{\rm h} - \psi_i)^2}{2\sigma_i^2}\right]\right) - \lambda_{\rm tar}\sin(\phi_{\rm h} - \psi_{\rm tar}), \quad (4)$$

where

$$\sigma_i = \arctan\left(\tan\left(\frac{\Delta\theta}{2}\right) + \frac{R_{\rm robot}}{R_{\rm robot} + d_i}\right). \quad (5)$$

where $\Delta\theta$ is the sensor angular resolution, $R_{\rm robot}$ is the radius of the robot, d_i is the distance to obstacles detected by sensor i, n_s is the number of sensors, $\lambda_{\rm tar}$ and $\lambda_{{\rm obs},i}$ define the strength of attraction and repulsion respectively.

C. Timing Control

The timing control is responsible for generating the linear velocity v for the robot through a Landau-Stuart oscillator that generates in real time the velocity profile for the robot (see [11]),

$$\dot{m} = \alpha\left(\mu - (m - O_{\rm m})\right)(m - O_{\rm m}) - \omega n, \quad (6)$$

$$\dot{n} = \alpha\left(\mu - (m - O_{\rm m})\right)n + \omega\,(m - O_{\rm m}), \quad (7)$$

where m and n are the state variables, ω specifies the frequency of oscillations, O_m controls the m solution offset and μ encodes the amplitude of the oscillations (see [15] for details).

The timing adaptation block is responsible for selecting the amplitude of the oscillations A and frequency ω. The task of reaching the goal location is subdivided into three time intervals, such their sum equals the movement time $MT(\mathrm{s})$. For each time interval the frequency of oscillation is defined as $\omega_1 = \frac{\pi}{2T_1}$, $\omega_2 = \frac{\pi}{T_2}$ and $\omega_3 = \frac{\pi}{2T_3}$ and the amplitudes as,

$$A_1 = \frac{D(t)}{\frac{\frac{\pi}{2}-1+\sin(\omega_1 t)}{\omega_1} + \frac{\pi+2}{\omega_2} + \frac{\frac{\pi}{2}-1}{\omega_3} - t}, \quad 0 < t \leq t_1, \quad (8)$$

$$A_2 = \frac{D(t)}{\frac{\frac{\pi}{2}}{\omega_1} + \frac{\pi+1+\cos(\omega_2(t-T_1))}{\omega_2} + \frac{\frac{\pi}{2}-1}{\omega_3} - t}, \quad t_1 < t \leq t_2, \quad (9)$$

$$A_3 = \frac{D(t)}{\frac{\frac{\pi}{2}}{\omega_1} + \frac{\pi}{\omega_2} + \frac{\frac{\pi}{2}-\cos(\omega_3(t-T_1-T_2))}{\omega_3} - t}, \quad t_2 < t \leq t_3. \quad (10)$$

The velocity profile is modulated in amplitude and frequency by simply changing both A and ω parameters respectively according to the current state as follows,

$$A'(\omega) = \frac{A_1(\omega_1)}{\left(1+e^{b(m-O_m)}\right)\left(1+e^{bn}\right)} + \frac{A_2(\omega_2)}{1+e^{-b(m-O_m)}} + \frac{A_3(\omega_3)}{\left(1+e^{b(m-O_m)}\right)\left(1+e^{-bn}\right)}, \quad (11)$$

where the values of A and ω alternate depending on the current values of m and n variables. The value of b controls the alternation speed between these values $(b = 500)$.

IV. Simulations

Here we describe some experiments realized in a simulated hospital environment using a Pioneer 3-DX robot. For simulating the experiments, the Webots simulated was used. The purpose of these experiments is to demonstrate the performance of our navigation architecture to generate timed trajectories for a mobile robot moving in a hospital environment. We assume that the uncertainty on the robot's localization is $\tau = 0.5(\mathrm{m})$, and $\varepsilon = 0.3(\mathrm{m})$, which is a sufficient distance that allows the robot to stop safely. To model the pedestrian walking behavior in the hospital environment, we used the social force model described in [8]

A. Simulation 1

In this simulation we intent to demonstrate that the mobile robot is able to circumnavigate people and other static obstacles found in hospital environments during a robotic mission. The robot has to reach the goal location in $MT = 120$ s while avoiding the obstacles located in the environment. Snapshots of the simulation are depicted in fig. 2.

The velocity profile v (blue line) and the amplitude A of the oscillator (green dashed line) are depicted in fig. 3 (top). There are obstacles that make the robot to decelerate its velocity $(t \approx 59(\mathrm{s}))$, $(t \approx 78(\mathrm{s}))$ and $(t \approx 88(\mathrm{s}))$ in order to ensure a safe circumnavigation. The deceleration of the robot's velocity

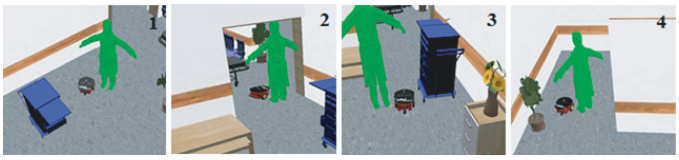

Fig. 2. Snapshots of simulation 1.

is achieved by decreasing the amplitude A of the oscillator. After the obstacle circumnavigation the amplitude increases to augment the velocity v and to compensate for the provoked delay, which allows the robot to reach the goal location within the specified movement time.

Fig. 3 (bottom) shows the direction ψ_{tar} (red dashed line) that the robot has to follow for reaching the goal location P_g and the direction that the robot follows ϕ_{h} (black dashed line) calculated by odometry. The robot follows ψ_{tar} excepting when it has to circumnavigate obstacles. After the obstacle circumnavigation the robot's heading direction ϕ_{h} converges to ψ_{tar}. In this simulation we verify that the robot is able to reach the goal location P_g within MT while avoiding

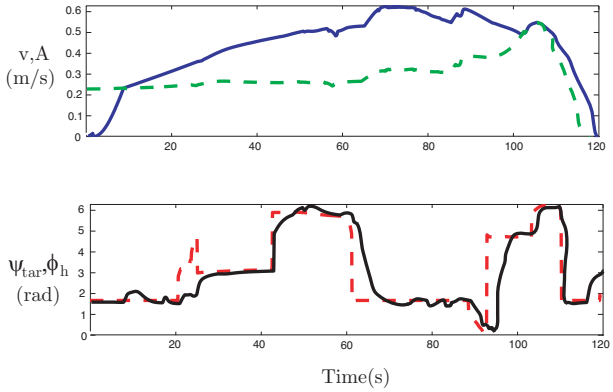

Fig. 3. Top) velocity v performed by the robot (blue line) and amplitude A of the oscillator (green dashed line). Bottom) Direction that the robot has to follow ψ_{tar} (red dashed line) and direction followed by the robot ϕ_{h} (black continuous line).

B. Simulation 2

In the second simulation, we intent to verify if the robot is able to circumnavigate typical obstacles of hospital environments while performing several missions in the specified movement time $MT(\mathrm{s})$ assigned to each mission. Herein, the robot executes 5 missions during approximately 350 s. Fig. 4 shows a sequence of snapshots obtained during the simulation where the robot faces different but typical situations in a hospital environment.

Fig. 5 (top) demonstrates the velocity v (blue line) of the robot during the 5 missions. Note that the robot accelerates when the missions are initiated and decelerates when it approaches the goal location until stopping. Fig. 5 (bottom) shows the distance D between the position of the robot P_{ro} and the goal location P_g. We can verify that the robot successfully reaches the goal location within the specified MT of each

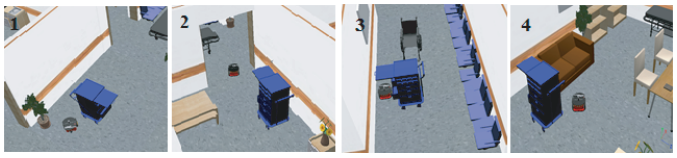

Fig. 4. Snapshots of simulation 2.

mission, since D is approximately 0 at the end of the respective mission.

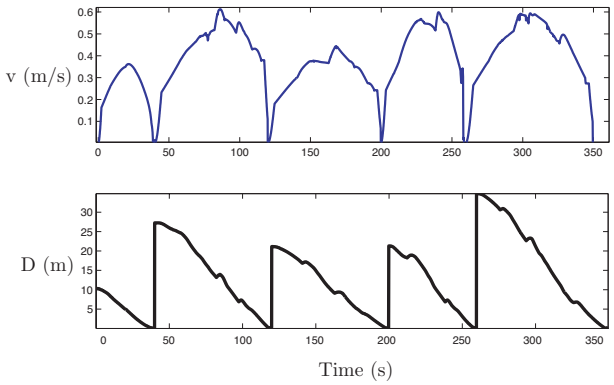

Fig. 5. Top) velocity v performed by the robot (blue line). Bottom) Distance D between the current position of the robot and the goal location (black line).

Fig. 6 demonstrates the limit-cycle of the Laudau-Stuart oscillator, where it is noticeable the several oscillations with different radius realized by the oscillator in order to generate the required velocity.

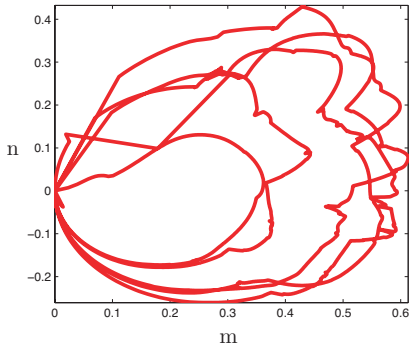

Fig. 6. Limit cycle of the Landau-Stuart oscillator.

V. CONCLUSIONS AND FUTURE WORKS

This paper presents a timing navigation architecture for mobile robots based on a mesh of nonlinear dynamical systems and feedthrough maps designed to control mobile robots for realizing tasks under timing constraints. The architecture is divided according to its level of abstraction similar to other architectures in the literature. The navigation architecture was successfully applied to a hospital delivery robot, since the robot realized its tasks of delivering goods between different locations of the hospital environment within the specified movement time to realize the respective task.

For future work we intent to validate the architecture in a real hospital environment.

ACKNOWLEDGMENT

Jorge Silva is supported by PhD Grant SFRH/BD/68805/2010. This work was supported by FEDER Funds and National Funds through FCT under the projects PEst-OE/EEI/LA0009/2011, PTDC/EEA-CRO/100655/2008 and FCOMP-01-FEDER-0124-022674.

REFERENCES

[1] Japancorp. [Online]. Available: http://www.japancorp.net, last visited on 14th of October, 2012

[2] Robocart from california computer research inc. [Online]. Available: http://www.robocart.com/, last visited on 14th of October, 2012

[3] Speciminder from ccsrobotisc. [Online]. Available: http://www.speciminder.com/, last visited on 14th of October, 2012

[4] Swisslog, switzerland. [Online]. Available: http://www.swisslog.com/, last visited on 14th of October, 2012

[5] Tug delivery system from aethon. [Online]. Available: http://www.aethon.com/, last visited on 14th of October, 2012

[6] E. Bicho, P. Mallet, and G. Schöner., "Target representation on an autonomous vehicle with low-level sensors." *The International Journal of Robotics Research*, no. 210, pp. 424–447, 2000.

[7] G. Engelberger, "Helpmate, a service robot with experience," *Industrial Robot*, vol. 25, no. 2, pp. 101–104, 1998.

[8] D. Helbing and P. Molnar, "Social force model for pedestrian dynamics," *PHYSICAL REVIEW E*, vol. 51, pp. 42–82, 1995. [Online]. Available: doi:10.1103/PhysRevE.51.4282

[9] A. J. Ijspeert, J. Nakanishi, and S. Schaal, "Learning attractor landscapes for learning motor primitives," in *Advances in Neural Information Processing Systems 15*. MIT Press, 2002, pp. 1547–1554.

[10] R. Ronsse, N. Vitiello, T. Lenzi, J. van den Kieboom, M. Carrozza, and A. Ijspeert, "Human-robot synchrony: flexible assistance using adaptive oscillators," *IEEE Transactions on Biomedical Engineering*, vol. 58, no. 4, pp. 1001–1012, 2011.

[11] C. Santos, "Generating timed trajectories for an autonomous vehicle: a non-linear dynamical systems approach." *in Proc. of the IEEE Int. Conf. on Robotics and Automation (ICRA)*, 2004.

[12] C. Santos and V. Matos, "Gait transition and modulation in a quadruped robot: A brainstem-like modulation approach," *Robotics and Autonomous Systems*, vol. 59, pp. 620–634, 2011.

[13] G. Schöner, "A dynamic theory of coordination of discrete movement," *in Biological Cybernetics*, vol. 63, pp. 257–270, 1990.

[14] J. Sequeira, C. Santos, and J. Silva, "Dynamical systems in robot control architectures: A building block perspective," *Proceedings of the 12th International Conference on Control, Automation, Robotics and Vision, ICARCV*, 2012.

[15] J. Silva, C. Santos, and V. Matos, "Timed trajectory generation for a toy-like wheeled robot," *In 36th Annual Conference of the IEEE Industrial Electronics Society, Glendale, USA, November 07-10*, pp. 1645 – 1650, 2010.

[16] T. Szecsi, K. A. Mamun, M. Hasan, A. Islam, C. Griffin, and A. Hoque, "Hospital robot module development in the iward project," *Interactive Systems in Healthcare*, 2010.

[17] M. Takahashi, T. Suzuki, H. Shitamoto, T. Moriguchi, and K. Yoshida, "Developing a mobile robot for transport applications in the hospital domain," *Robotics and Autonomous Systems*, vol. 58, pp. 889 – 899.

[18] S. Thrun, "Learning metric-topological maps for indoor mobile robot navigation," in *Artificial Intelligence*, vol. 99, no. 1, 1998, pp. 21 – 71.